


## Article

# An Enhanced DOA Estimation Method for Coherent Sources via Toeplitz Matrix Reconstruction and Khatri–Rao Subspace

Bingbing Qi <sup>1</sup> , Xiaogang Liu <sup>1</sup>, Daowei Dou <sup>1</sup>, Yan Zhang <sup>2</sup> and Runze Hu <sup>1,\*</sup>

<sup>1</sup> School of Information and Electronics, Beijing Institute of Technology, Beijing 100080, China; 6120230031@bit.edu.cn (B.Q.); yingjxt@163.com (X.L.); ddw@bit.edu.cn (D.D.)

<sup>2</sup> School of Computer Science, Xiamen University, Xiamen 361000, China; bzhy986@gmail.com

\* Correspondence: hrzlpk2015@gmail.com

**Abstract:** The Toeplitz matrix reconstruction methods are capable of resolving coherent signals, playing a crucial role in the direction-of-arrival (DOA) estimation of acoustic sources. However, the decoherence processing sacrifices the array aperture and further results in a reduced resolution capability for the number of identifiable sources. To solve this issue, we propose an enhanced method using the Khatri–Rao subspace to resolve more coherent sources than that of the existing Toeplitz matrix reconstruction methods. Firstly, a full set of Toeplitz matrices with full rank is obtained. Then, the virtual array aperture can be obtained using the Khatri–Rao product of the array response, and the degree of freedom provided inherently in the virtual array structure is about twice the size of that of the existing Toeplitz methods. Next, linear processing is further used to achieve complexity reduction without losing the effective degree of freedom. Finally, the DOA estimation for more coherent sources can be achieved by combining it with conventional methods. Numerical simulations verify the superiority of the proposed method.

**Keywords:** DOA; Khatri–Rao product; coherent signals; virtual array



**Citation:** Qi, B.; Liu, X.; Dou, D.; Zhang, Y.; Hu, R. An Enhanced DOA Estimation Method for Coherent Sources via Toeplitz Matrix Reconstruction and Khatri–Rao Subspace. *Electronics* **2023**, *12*, 4268. <https://doi.org/10.3390/electronics12204268>

Academic Editors: Stefanos Kollias, Shaohui Lin, Fuhai Chen and Yunhang Shen

Received: 8 September 2023

Revised: 7 October 2023

Accepted: 10 October 2023

Published: 16 October 2023



**Copyright:** © 2023 by the authors. Licensee MDPI, Basel, Switzerland. This article is an open access article distributed under the terms and conditions of the Creative Commons Attribution (CC BY) license (<https://creativecommons.org/licenses/by/4.0/>).

## 1. Introduction

The ocean is a vast and largely unexplored frontier, replete with an abundance of resources within its aquatic realm. This circumstance has engendered an escalating demand for the development of underwater sensing and communication systems, based upon advanced multimedia information processing technologies. Central to the functionality of these systems is the process of direction-of-arrival (DOA) estimation, which serves as the linchpin for source localization, beamforming, and target tracking [1–5]. In practice, coherent signal sources are usually encountered owing to multipath propagation or various interference [6,7]. In such cases, the subspace-based methods such as estimation of signal parameters via invariance techniques (ESPRIT) [8] and multiple signal classification (MUSIC) [9] will suffer from performance degradation owing to the rank deficiency in the source covariance matrix. To restore its rank, the methods based on spatial smoothing were developed to solve this problem [10–15]. However, because of the reduced array aperture in the overlapped subarrays, a common drawback is that they reduce the ability to identify the source number that can be resolved.

Methods such as maximum likelihood [16] and subspace fitting [17] have been proposed to resolve coherent sources. The coherent DOA estimation problem can be achieved via multi-dimensional parameter optimization without using eigenvalue decomposition. Thus, they are insensitive to signal coherence. However, the optimal solution is obtained via alternating maximization, which further results in computational burden. Meanwhile, compressed sensing methods [18–20] have been developed for coherent signal DOA estimation. These methods exploit the spatial sparse characteristics of the source signals and then solve the coherent signal DOA estimation through sparse vector recovery. However, the optimal solution needs to be implemented interactively, which results in high

computational complexity. The high-order cumulants methods [21,22] have also been employed to resolve the coherent signals, which produce better estimation performance because of the enhanced noise suppression ability. Meanwhile, this process can produce an extended virtual array that can distinguish more sources. Nonetheless, the high-order cumulants estimation accuracy usually requires more snapshots and further results in increased computational complexity.

Recently, the idea of the so-called Toeplitz matrix reconstruction technique with moderate computational cost was also proposed to obtain the DOA estimation of the coherent sources [23–26]. The source covariance matrix in the reconstructed Toeplitz matrix corresponding to its row vector of the array output covariance matrix is a diagonal matrix with the restored full rank. Then, the DOAs are obtained by combining with conventional subspace-based methods. In [27], the beamspace-based Toeplitz matrix reconstruction method based on beamspace processing was proposed for its noise suppression ability. Furthermore, it performs better estimation in cases of a low SNR regime. However, similar to spatial smoothing methods, the existing Toeplitz matrix reconstruction methods realize the signal decorrelation at the cost of reducing the array aperture, which further results in resolution capability degradation for resolving more source signals.

To address the aforementioned problems, an enhanced coherent DOA estimation method via Toeplitz matrix reconstruction and Khatri–Rao subspace is designed to resolve more sources. Firstly, a set of Toeplitz matrices associated with each row vector of the array output covariance matrix is constructed, and then the reconstructed matrices are vectored and stacked to achieve the covariance matrix reconstruction of the array output. Furthermore, the virtual array aperture for the proposed method is about twice as big as that of the existing Toeplitz matrix methods, which further provides us with the capability of resolving more sources. Next, linear processing is employed to reduce the dimension, which leads to a lower computational cost in implementation. Meanwhile, it also achieves noise-whitening processing. In the end, the estimated DOA of coherent sources can be obtained via the conventional subspace-based methods. Numerical results also show that the proposed method can resolve more sources compared to the existing methods.

This paper is structured as follows: Sections 2 and 3 present the signal model and the existing method, and the hypothesis proposed in this paper is further introduced in Section 4. In Section 5, several analysis experiments are then presented. Finally, the paper is concluded in Section 6.

Notation:  $(\cdot)^H$  represents conjugate transpose,  $(\cdot)^T$  denotes transpose,  $(\cdot)^*$  is conjugate.  $\mathbf{X}$ ,  $\mathbf{x}$ , and  $x$  denote the matrix, vector, and scalar, respectively.  $E[\cdot]$  is the expectation operation.  $\mathbf{I}_M$  denotes  $M \times M$  identity matrix.

### 2. Signal Model

Consider a uniform linear array (ULA) that contains  $N = 2M + 1$  sensors with half-wavelength ( $d = \lambda/2$ ) as shown in Figure 1, and  $P$  narrowband far-field signals with distinct directions  $\theta_i, i = 1, 2, \dots, P$  are received by the array. Moreover, the complex envelope for source signals can be denoted as  $s_i(t), i = 1, 2, \dots, P$  at the sensor 0, which is set as the reference.

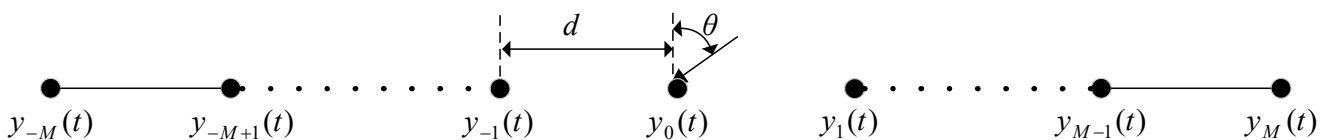


Figure 1. Antenna array model.

The array output vector  $\mathbf{y}(t)$  at time  $t$  can be written as

$$\begin{aligned} \mathbf{y}(t) &= [y_{-M}(t), \dots, y_0(t), \dots, y_M(t)]^T \\ &= \mathbf{x}(t) + \mathbf{n}(t) \\ &= \mathbf{A}\mathbf{s}(t) + \mathbf{n}(t) \end{aligned} \tag{1}$$

where the  $\mathbf{s}(t) = [s_1(t), \dots, s_P(t)]^T$  denotes  $P \times 1$  source vector. The  $(2M + 1) \times P$  array steering matrix is expressed as  $\mathbf{A} = [\mathbf{a}(\theta_1), \dots, \mathbf{a}(\theta_P)]$  with the  $i$ -th steering vector  $\mathbf{a}(\theta_i) = [e^{-j(2\pi/\lambda)Md \sin \theta_i}, \dots, 1, \dots, e^{j(2\pi/\lambda)Md \sin \theta_i}]^T$ .  $\mathbf{n}(t) = [n_{-M}(t), \dots, n_M(t)]^T$  represents the  $(2M + 1) \times 1$  noise vector with Gaussian white characteristics which are assumed to be uncorrelated to signal sources with zero mean and variance  $\sigma_n^2$ .

Based on the assumptions described in (1), the covariance matrix of the array output  $\mathbf{R}$  can be expressed as

$$\begin{aligned} \mathbf{R} &= E[\mathbf{y}(t)\mathbf{y}^H(t)] \\ &= \mathbf{A}E[\mathbf{s}(t)\mathbf{s}^H(t)]\mathbf{A}^H + E[\mathbf{n}(t)\mathbf{n}^H(t)] \\ &= \mathbf{A}\mathbf{R}_s\mathbf{A}^H + \sigma_n^2\mathbf{I}_{(2M+1)} \end{aligned} \tag{2}$$

where  $\mathbf{R}_s = E[\mathbf{s}(t)\mathbf{s}^H(t)]$  is the  $P \times P$  source covariance matrix. When performing eigen-decomposition, the rank loss of the matrix  $\mathbf{R}_s$  will result in performance degradation in DOA estimation or even failure [12,13]. Therefore, the key processing for the coherent DOA estimation when combined with the subspace-based methods is to restore the rank of the source covariance matrix [25–27].

### 3. Toeplitz Matrix Reconstruction Method

The Toeplitz matrix reconstruction methods [24–27] exploit a set of Toeplitz matrices with restored rank associated with row vectors to achieve the matrix reconstruction of the array output which restores the rank of the source covariance matrix. Thus, the DOAs of sources can be further obtained when using the subspace-based methods. In a manner akin to spatial smoothing techniques, the Toeplitz matrix reconstruction process also reduces the array aperture, resulting in a decrease in resolution for more signals.

Using the result in [26], the reconstructed matrix  $\mathbf{R}_{Y_i}$  with full rank corresponding to the  $i$ -th row vector of the array output covariance matrix  $\mathbf{R}$  is given as

$$\begin{aligned} \mathbf{R}_{Y_i} &= E[\mathbf{R}_Y(t)y_i^*(t)] \\ &= E[\mathbf{R}_X(t)x_i^*(t)] + E[\mathbf{R}_N(t)n_i^*(t)] \\ &= \mathbf{R}_{X_i} + \sigma_n^2\tilde{\mathbf{I}}_{(M+1),i} \end{aligned} \tag{3}$$

$$\begin{aligned} \mathbf{R}_Y(t) &= \begin{bmatrix} y_0(t) & y_1(t) & \dots & y_M(t) \\ y_{-1}(t) & y_0(t) & \dots & y_{M-1}(t) \\ \vdots & \vdots & \ddots & \vdots \\ y_{-M}(t) & y_{-M+1}(t) & \dots & y_0(t) \end{bmatrix} \\ &= \mathbf{R}_X(t) + \mathbf{R}_N(t) \end{aligned} \tag{4}$$

$$\begin{aligned} \mathbf{R}_X(t) &= \begin{bmatrix} x_0(t) & x_1(t) & \dots & x_N(t) \\ x_{-1}(t) & x_0(t) & \dots & x_{N-1}(t) \\ \vdots & \vdots & \ddots & \vdots \\ x_{-N}(t) & x_{-N+1}(t) & \dots & x_0(t) \end{bmatrix} \\ &= \tilde{\mathbf{A}}\mathbf{S}(t)\tilde{\mathbf{A}}^H \end{aligned} \tag{5}$$

$$\mathbf{R}_N(t) = \begin{bmatrix} n_0(t) & n_1(t) & \cdots & n_N(t) \\ n_{-1}(t) & n_0(t) & \cdots & n_{N-1}(t) \\ \vdots & \vdots & \ddots & \vdots \\ n_{-N}(t) & n_{-N+1}(t) & \cdots & n_0(t) \end{bmatrix} \tag{6}$$

where  $\mathbf{R}_Y(t)$  is the reconstructed  $(M + 1) \times (M + 1)$  Toeplitz matrix via  $\mathbf{y}(t)$ .  $\mathbf{R}_X(t)$  and  $\mathbf{R}_N(t)$  denotes the reconstructed signal matrix and noise matrix with Toeplitz characteristics, respectively.  $\tilde{\mathbf{A}} = [\tilde{\mathbf{a}}(\theta_1), \dots, \tilde{\mathbf{a}}(\theta_P)]$  represents the  $(M + 1) \times P$  array steering matrix with  $\tilde{\mathbf{a}}(\theta_i) = [1, \dots, e^{-j(2\pi/\lambda)Md \sin \theta_i}]^T$  corresponding to the reconstructed matrix  $\mathbf{R}_X(t)$ , and  $\mathbf{S}(t) = \text{diag}\{s_1(t), \dots, s_P(t)\}$  is the reconstructed  $P \times P$  source covariance matrix containing each signal on its diagonal elements.

Furthermore, the reconstructed correlation matrix based on  $\mathbf{R}_X(t)$  and  $x_i(t)$  can be given by [24]

$$\mathbf{R}_{Xi} = E[\mathbf{R}_X(t)x_i^*(t)] = \tilde{\mathbf{A}}E[\mathbf{S}(t)x_i^*(t)]\tilde{\mathbf{A}}^H = \tilde{\mathbf{A}}\tilde{\mathbf{S}}_i\tilde{\mathbf{A}}^H \tag{7}$$

where  $\tilde{\mathbf{S}}_i$  denotes the correlation matrix between  $\mathbf{S}(t)$  and the obtained signal from the  $i$ -th sensor.

In a similar way, the reconstructed matrix  $\mathbf{R}_{Yi}$  under a noise field can be written as

$$\mathbf{R}_{Yi} = \tilde{\mathbf{A}}E[\mathbf{S}(t)x_i^*(t)]\tilde{\mathbf{A}}^H + \sigma_n^2\tilde{\mathbf{I}}_{(M+1),i} = \tilde{\mathbf{A}}\tilde{\mathbf{S}}_i\tilde{\mathbf{A}}^H + \sigma_n^2\tilde{\mathbf{I}}_{(M+1),i} \tag{8}$$

We can conclude from (3) and (8) that the Toeplitz matrix processing named the ESPRIT-like method transforms the source matrix  $\mathbf{R}_s$  described in (1) to a diagonal matrix  $\tilde{\mathbf{S}}_i$  with restored full rank described in (7) to achieve signal decoherence. Then, the coherent DOAs can be obtained using the conventional subspace-based methods. However, the matrix reconstruction process reduces the effective aperture of the array since the dimension of the reconstructed matrix  $\mathbf{R}_{Yi}$  is smaller than that of the original matrix  $\mathbf{R}$ , which further reduces the ability to identify the sources that can be resolved.

To avoid only employing partial information of the covariance matrix of the array output in the ESPRIT-like method, many enhanced methods including the forward and backward partial Toeplitz matrices reconstruction named FB-PTMR [24] and the multiple Toeplitz matrices reconstruction called MTOEP [25] were proposed to employ more information to achieve the matrix reconstruction. Thus, they can produce a better estimation of the reconstructed matrix and then improve the DOA estimation performance. The reconstructed covariance matrix of the array output for the FB-PTMR and MTOEP can be expressed as

$$\mathbf{R}_{FP-PTMR} = \sum_{i=0}^M \mathbf{R}_{Yi}\mathbf{R}_{Yi}^H \tag{9}$$

$$\mathbf{R}_{MTOEP} = \sum_{i=-M}^M \mathbf{R}_{Yi}\mathbf{R}_{Yi}^H \tag{10}$$

We can observe from (9) and (10) that the improved methods employ a set of Toeplitz matrices corresponding to several rows to reconstruct the covariance matrix of the array output through quadratic spatial smoothing. However, similar to the ESPRIT-like method, the reconstructed covariance matrix of the array output for the FB-PTMR and MTOEP methods still have the  $(M + 1) \times (M + 1)$  characteristics. Thus, this will result in a reduced number of distinguishable signal sources.

#### 4. The Proposed Method

To resolve more source signals, an enhanced DOA estimation method for coherent sources via Toeplitz matrix reconstruction and Khatri–Rao subspace is proposed. We

first construct a full set of Toeplitz matrices with restored rank, and then the Khatri–Rao processing is further employed to achieve the aperture extension of the reconstructed matrix. Therefore, it improves the ability to resolve more coherent signals than that of the existing ESPRIT-like method.

4.1. Khatri–Rao Processing Criterion

Firstly, similar to the vectorization process in [28,29], the reconstructed covariance matrix of the array output shown in (8) can be rewritten as

$$\mathbf{y}_i \triangleq \text{vec}\{\mathbf{R}_{Y_i}\} = (\tilde{\mathbf{A}}^* \odot \tilde{\mathbf{A}})\mathbf{d}_i + \text{vec}\left\{\sigma_n^2 \tilde{\mathbf{I}}_{(M+1),i}\right\} \tag{11}$$

where  $\mathbf{d}_i = [E[s_1(t)x_i^*(t)], \dots, E[s_P(t)x_i^*(t)]]^T$  is the  $P \times 1$  source vector for the reconstructed matrix;  $\mathbf{y}_i$ ;  $\text{vec}\{\cdot\}$  denotes vectorization.  $\odot$  represents the Khatri–Rao product. Then, when stacking  $\mathbf{Y} \triangleq [\mathbf{y}_M, \dots, \mathbf{y}_0, \dots, \mathbf{y}_{-M}]$ , we obtain

$$\begin{aligned} \mathbf{Y} &\triangleq [\mathbf{y}_M, \dots, \mathbf{y}_0, \dots, \mathbf{y}_{-M}] \\ &= (\tilde{\mathbf{A}}^* \odot \tilde{\mathbf{A}})[\mathbf{d}_M, \dots, \mathbf{d}_0, \dots, \mathbf{d}_{-M}] \\ &\quad + \sigma_n^2 [\text{vec}\{\tilde{\mathbf{I}}_{(M+1),M}\}, \dots, \text{vec}\{\tilde{\mathbf{I}}_{(M+1),0}\}, \dots, \text{vec}\{\tilde{\mathbf{I}}_{(M+1),-M}\}] \\ &= (\tilde{\mathbf{A}}^* \odot \tilde{\mathbf{A}})\boldsymbol{\psi} + \sigma_n^2 \mathbf{G} \end{aligned} \tag{12}$$

where  $\tilde{\mathbf{A}}^* \odot \tilde{\mathbf{A}}$  is the virtual array steering response.  $\boldsymbol{\psi}$  denotes the  $P \times (2M + 1)$  signal matrix.  $\mathbf{G}$  is the  $(M + 1)^2 \times (2M + 1)$  noise matrix.  $\boldsymbol{\psi}$  and  $\mathbf{G}$  have the following expressions

$$\begin{aligned} \boldsymbol{\psi} &= [\mathbf{d}_M, \dots, \mathbf{d}_0, \dots, \mathbf{d}_{-M}] \\ &= \begin{bmatrix} E[s_1(t)x_M^*(t)] & E[s_1(t)x_{M-1}^*(t)] & \dots & E[s_1(t)x_{-M}^*(t)] \\ E[s_2(t)x_M^*(t)] & E[s_2(t)x_{M-1}^*(t)] & \dots & E[s_2(t)x_{-M}^*(t)] \\ \vdots & \vdots & \ddots & \vdots \\ E[s_P(t)x_M^*(t)] & E[s_P(t)x_{M-1}^*(t)] & \dots & E[s_P(t)x_{-M}^*(t)] \end{bmatrix} \end{aligned} \tag{13}$$

$$\begin{aligned} \mathbf{G} &= [\text{vec}\{\tilde{\mathbf{I}}_{(M+1),M}\}, \dots, \text{vec}\{\tilde{\mathbf{I}}_{(M+1),0}\}, \dots, \text{vec}\{\tilde{\mathbf{I}}_{(M+1),-M}\}] \\ &= \begin{bmatrix} 0 \dots 0 & 1 & 0 & \dots & 0 \\ 0 \dots 0 & 0 & 1 & \dots & 0 \\ \vdots & \vdots & \vdots & \ddots & \vdots \\ 0 \dots 0 & 0 & 0 & \dots & 1 \\ \hline 0 \dots 1 & 0 & 0 & \dots & 0 \\ 0 \dots 0 & 1 & 0 & \dots & 0 \\ \vdots & \vdots & \vdots & \ddots & \vdots \\ 0 \dots 0 & 0 & \dots & 1 & 0 \\ \hline \vdots & \vdots & \vdots & \vdots & \vdots \\ 1 & 0 & \dots & 0 & \dots & 0 \\ 0 & 1 & \dots & 0 & \dots & 0 \\ \vdots & \vdots & \vdots & \vdots & \vdots & \vdots \\ 0 & 0 & \dots & 1 & 0 & \dots & 0 \end{bmatrix} \end{aligned} \tag{14}$$

#### 4.2. The Number of Sources Which Can Be Estimated

It has been proven in [28] that for  $\tilde{\mathbf{A}} \in C^{(M+1) \times P}$  as described in (12), the Khatri–Rao product  $\tilde{\mathbf{A}}^* \odot \tilde{\mathbf{A}}$  is a full-column rank matrix assuming that the source number satisfies  $P \leq 2M + 1$ . That is

$$\text{Rank} \left\{ \tilde{\mathbf{A}}^* \odot \tilde{\mathbf{A}} \right\} = P \tag{15}$$

where  $\text{Rank}\{\cdot\}$  denotes the standard rank.

Furthermore, using the result in [28], the signal matrix  $\boldsymbol{\psi} \in C^{P \times (2M+1)}$  can maintain a full rank assuming that the source power distributions over the columns are different and the source number satisfies  $P \leq 2M$ . The  $i$ -th row for the matrix  $\boldsymbol{\psi}$  in (13) can be written as

$$\boldsymbol{\psi}_i = [E[s_i(t)x_M^*(t)], E[s_i(t)x_{M-1}^*(t)], \dots, E[s_i(t)x_{-M}^*(t)]] \tag{16}$$

Firstly, substituting (1) into (16), we have

$$\boldsymbol{\psi}_i = \left[ \sum_{l=1}^P E[s_i(t)s_l^*(t)]e^{j(2\pi/\lambda)Md \sin \theta_l}, \dots, \sum_{l=1}^P E[s_i(t)s_l^*(t)]e^{-j(2\pi/\lambda)Md \sin \theta_l} \right] \tag{17}$$

Note that as defined in (1), because the source DOAs are distinct ( $\theta_i \neq \theta_j, i \neq j$ ), the source power distributions within the vector  $\boldsymbol{\psi}_i$  are different. Meanwhile, by combining the assumption  $P \leq 2M$  as shown in (16), the reconstructed source matrix  $\boldsymbol{\psi}$  is of full-column rank [28,29], which has the following expression

$$\text{Rank}\{\boldsymbol{\psi}\} = P \tag{18}$$

Then, inserting (15) and (18) into (12), we have the following expression [28,29]

$$\text{Rank}\{\mathbf{Y}\} = \text{Rank} \left\{ \tilde{\mathbf{A}}^* \odot \tilde{\mathbf{A}} \right\} = P \tag{19}$$

When performing the singular value decomposition (SVD), we obtain

$$\mathbf{Y} = [\mathbf{U}_s \ \mathbf{U}_n] \begin{bmatrix} \boldsymbol{\Sigma}_s & \mathbf{0} \\ \mathbf{0} & \mathbf{0} \end{bmatrix} \begin{bmatrix} \mathbf{V}_s^H \\ \mathbf{V}_n^H \end{bmatrix} \tag{20}$$

where  $\mathbf{U}_n \in C^{(M+1)^2 \times ((M+1)^2 - P)}$  is the left singular matrices associated with zero singular values, and  $\mathbf{V}_n \in C^{(2M+1) \times ((M+1)^2 - P)}$  denotes its corresponding right singular matrices. Meanwhile,  $\mathbf{U}_s \in C^{(M+1)^2 \times P}$  and  $\mathbf{V}_s \in C^{(2M+1) \times P}$  represent the left and right matrices corresponding to their nonzero singular values, respectively.  $\boldsymbol{\Sigma}_s \in R^{P \times P}$  is a diagonal matrix that contains nonzero singular values.

According to the array signal processing theory in [1,8,9], we have

$$R \left( \left( \tilde{\mathbf{A}}^* \odot \tilde{\mathbf{A}} \right)^\perp \right) = R(\mathbf{U}_s^\perp) = R(\mathbf{U}_n) \tag{21}$$

where  $R(\cdot)$  represents the range space.

Finally, the estimated DOAs can be derived as follows

$$\mathbf{U}_n^\perp \left[ \tilde{\mathbf{A}}^* \odot \tilde{\mathbf{A}} \right]_k = \mathbf{U}_n^\perp \left( \tilde{\mathbf{a}}^*(\theta_k) \otimes \tilde{\mathbf{a}}(\theta_k) \right) = 0 \tag{22}$$

where  $\otimes$  denotes the Kronecker product.

By employing the conclusions in [28,29], the actual angles  $\theta_k, k = 1, 2, \dots, P$  via the criterion in (22) based on Khatri–Rao processing can be estimated when the number of source signals  $P$  satisfy

$$P \leq 2(M + 1) - 2 \triangleq 2M \tag{23}$$

From (8)–(10) and (23), we can conclude that the maximum number of sources that can be resolved in our proposed method, given by  $2M$ , are greater than that of the existing Toeplitz matrix, which is  $M$ . This is because of the proposed method based on Khatri–Rao subspace processing, which can extend the array aperture as shown in (12).

### 4.3. Dimension Reduction

It can be seen in (12) and (22) that the array dimension in our proposed method, given by  $(M + 1)^2$ , is greater than the existing Toeplitz-based methods [23–27], that is  $(M + 1)$ , which increased the computational burden when it is combined with subspace-based methods. Furthermore, the noise contribution non-scalar matrix  $\mathbf{G}$  in (14) needs to be further processed, which also impacts the computational efficiency. For these problems, we can solve them by performing linear processing on the reconstructed matrix  $\mathbf{Y}$ , which reduces the dimension and further achieves complexity reduction. Meanwhile, the noise is also whitened during this processing. Therefore, the proposed method does not require noise elimination, making it less computationally complex.

Firstly, according to the reference [29], the virtual array response matrix  $\tilde{\mathbf{A}}^* \odot \tilde{\mathbf{A}}$  in (12) can be computed as follows

$$\tilde{\mathbf{A}}^* \odot \tilde{\mathbf{A}} = \mathbf{G}\mathbf{B} \tag{24}$$

where  $\mathbf{B} = [\mathbf{b}(\theta_1), \mathbf{b}(\theta_2), \dots, \mathbf{b}(\theta_P)]$  denotes the  $(2M + 1) \times P$  dimension-reduced array steering matrix with  $\mathbf{b}(\theta_i) = [e^{-j(2\pi/\lambda)Md \sin \theta_i}, \dots, 1, \dots, e^{j(2\pi/\lambda)Md \sin \theta_i}]^T$ .

Then, substituting (24) into (12), the reconstructed matrix  $\mathbf{Y}$  can be rewritten as

$$\mathbf{Y} = \mathbf{G}\mathbf{B}\boldsymbol{\psi} + \sigma_n^2 \mathbf{G} \tag{25}$$

where  $\sigma_n^2$  denotes the noise energy.

Next, it can be verified from (14) that the column vectors contained in the matrix  $\mathbf{G}$  with full-column rank are orthogonal. Thus, the diagonal matrix  $\mathbf{W}$  can be further obtained, which has the following expression [29]

$$\mathbf{W} = \mathbf{G}^T \mathbf{G} = \text{diag}\{1, 2, \dots, M, M + 1, M, \dots, 2, 1\} \tag{26}$$

By combining (25) and (26), the reconstructed matrix with dimension reduction can be achieved through a linear operation [29]. We can write that

$$\begin{aligned} \tilde{\mathbf{Y}} &= \mathbf{W}^{-1} \mathbf{G}^T \mathbf{Y} \\ &= \mathbf{W}^{-1} \mathbf{G}^T (\mathbf{G}\mathbf{B}\boldsymbol{\psi} + \sigma_n^2 \mathbf{G}) \\ &= \mathbf{W}^{-1} \mathbf{G}^T \mathbf{G}\mathbf{B}\boldsymbol{\psi} + \sigma_n^2 \mathbf{W}^{-1} \mathbf{G}^T \mathbf{G} \\ &= \mathbf{B}\boldsymbol{\psi} + \sigma_n^2 \mathbf{I}_{(2M+1)} \end{aligned} \tag{27}$$

According to the results from (12) and (27), when performing linear processing, the reconstructed matrix is transformed from  $\mathbf{Y} \in C^{(M+1)^2 \times (2M+1)}$  into  $\tilde{\mathbf{Y}} \in C^{(2M+1) \times (2M+1)}$ , which significantly reduces the complexity burden in implementations without losing the effective degree. Meanwhile, noise-whiten processing is also achieved, which further results in better DOA estimation accuracy than that in color-noise cases [30–32].

The auto-correlation and spatial smoothing for the dimension-reduced matrix  $\tilde{\mathbf{Y}}$  are employed to improve the noise suppression ability [26,33]. We obtain

$$\tilde{\mathbf{R}} = \tilde{\mathbf{Y}}\tilde{\mathbf{Y}}^H \tag{28}$$

$$\mathbf{R}_{proposed} = \tilde{\mathbf{R}} + \mathbf{J}(\tilde{\mathbf{R}})^* \mathbf{J} \tag{29}$$

where  $\mathbf{J}$  is the exchange matrix.

Finally, the DOAs for coherent sources can be estimated via the total least squares ESPRIT (TLS-ESPRIT) method [34].

The major steps of the proposed method are summarized in Algorithm 1.

---

**Algorithm 1:** Pseudocode of the proposed DOA estimation method

---

**Input:** Array output vector,  $\mathbf{y}(t)$ .

**Output:** Estimated signal source DOAs,  $\theta_d, d = 1, \dots, P$ .

- 1: Apply  $\mathbf{R} = \sum_{l=1}^L \mathbf{y}(t)\mathbf{y}^H(t)$  instead of (2) to calculate the output covariance matrix.
  - 2: Construct the Toeplitz matrix  $\mathbf{R}_{Y_i}, i = -M, \dots, M$  with full rank corresponding to the  $i$ -th row vector of the covariance matrix  $\mathbf{R}$  using (3).
  - 3: Perform the Khatri–Rao processing criterion to obtain the reconstructed matrix with aperture extension  $\mathbf{Y}$  using (11) and (12).
  - 4: The reconstructed matrix  $\tilde{\mathbf{Y}}$  with dimension reduction is obtained using (25)–(27).
  - 5: Obtain the reconstructed covariance  $\mathbf{R}_{proposed}$  with better noise suppression ability using (28) and (29).
  - 6: Perform TLS-ESPRIT (total least squares ESPRIT) to estimate the DOAs of the signal sources.
- 

For the TLS-ESPRIT method, the computational complexity of our proposed method mainly lies in the calculation of  $\mathbf{Y}$ , dimension reduction, and DOA estimation. Thus, we add these processes to obtain the computational burden.  $2M + 1$  denotes the number of elements in the array,  $L$  represents the snapshot number,  $X$  denotes the smoothing number of FOSS/FBSS methods, and  $P$  represents the number of source signals. The main computational complexities of these methods are shown in Table 1.

**Table 1.** Computational complexity analysis.

Algorithm	Computational Complexity
FOSS/FBSS	$O\left((2M + 1)^2L + (2M - X + 2)^3 + 3(2M - X + 1)P^2 + 2P^3\right)$
FB-PTMR	$O\left((2M + 1)^2L + (M + 1)^4 + (M + 1)^3 + 3MP^2 + 2P^3\right)$
MTOEP	$O\left((2M + 1)^2L + (M + 1)^3(2M + 1) + (M + 1)^3 + 3MP^2 + 2P^3\right)$
ESPRIT-like	$O\left((2M + 1)^2L + (M + 1)^3 + 3MP^2 + 2P^3\right)$
The proposed method	$O\left((2M + 1)^2L + (2M + 1)^2(M + 1)^2 + (2M + 1)^3 + 3(2M + 1)P^2 + 2P^3\right)$

Compared with the existing Toeplitz and spatial smoothing methods, our proposed method exploits the Khatri–Rao processing to achieve the aperture extension of the reconstructed matrix, which increases the computational burden. However, it can provide the capability to identify more sources. Meanwhile, the DOA estimation performance is also improved.

In addition, the proposed method in this paper mainly emphasizes that the array aperture extension can be achieved by combing with Khatri–Rao subspace processing, and further provides better DOA estimation accuracy in cases of low SNR when compared to the existing Toeplitz matrix reconstruction methods. Moreover, the aperture extension essentially provides us with the ability to resolve more source signals than that of the existing Toeplitz matrix reconstruction methods. For simplicity of analysis, we select the ESPRIT-like [23] method as an estimator to reflect the advantages of Khatri–Rao subspace processing. Thus, when combined with another high resolution-method [26,27,30], it



will also provide better performance on estimation and resolution. The DOA estimation performance is also affected by element spacing, array patterns, and mutual coupling [1,2,7]. However, this paper mainly focuses on the advantages of Khatri–Rao subspace processing. Thus, DOA estimation under these conditions will be the topic of our future research.

### 5. Simulation Results

Numerical simulations are presented to illustrate the superiority of our proposed method compared with the spatial smoothing methods including FBSS [11], FOSS [10], and the Toeplitz reconstruction methods such as MTOEP [25], ESPRIT-like [23], and FB-PTMR [24] based on the basis of the probability of resolution (POR) and the root-mean-square error (RMSE). The RMSE and POR of the DOA estimates are defined as

$$RMSE = \sqrt{\frac{1}{WP} \sum_{i=1}^P \sum_{w=1}^W (\tilde{\theta}_{i,w} - \theta)^2} \tag{30}$$

$$POR = \left( \frac{1}{WP} \sum_{i=1}^P N_i \right) \times 100\% \tag{31}$$

where  $W$  represents the Monte Carlo trial number, which is set to 2000 in our simulations.  $\tilde{\theta}_{i,w}$  is the  $i$ -th estimated value of  $\theta_i$  in the  $w$ -th trial.  $P$  denotes the source number assumed to be known or accurately estimated [35–37]. The resolution is considered successful when the estimated value satisfies  $|\tilde{\theta}_{i,w} - \theta| \leq 2^\circ$ , and  $N_i$  counts the number of successful resolutions for the  $i$ -th signal source.

#### 5.1. Estimated Source Number Verification

Firstly, we verify the maximum source number that can be resolved for our proposed method. As shown in Figure 2, the case where  $(N, P) = (5, 4)$  is considered. A group of two coherent sources located at  $[-40^\circ, -20^\circ]$  and another group contains two coherent sources received from  $[10^\circ, 45^\circ]$ . The spacing between the adjacent elements is half-wavelength ( $d = \lambda/2$ ), and the number of snapshots is 200. The noise is zero-mean white Gaussian with power  $\sigma_n^2$  and the SNR varies from  $-10$  dB to  $12$  dB according to  $SNR = 10 \log(\sigma_n^{-2})$  [38].

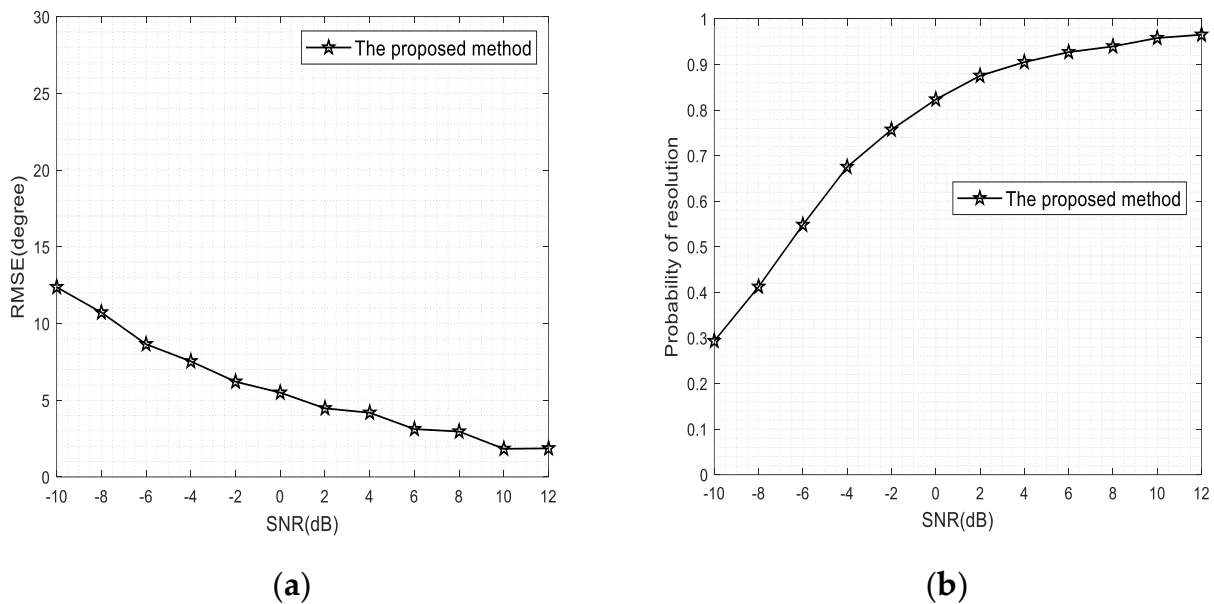


Figure 2. DOA estimation performance in  $(N, P) = (5, 4)$  case. (a) RMSE versus SNR. (b) POR versus SNR.

The existing spatial smoothing and Toeplitz matrix reconstruction methods can not resolve the coherent sources under this condition. However, our proposed method is still able to identify the sources because our proposed method exploits the Khatri–Rao subspace processing that provides an extended virtual array, which is consistent with the analysis in Section 4. Thus, our proposed method provides the ability to resolve the angle estimation problem for more signals.

### 5.2. Estimation Performance versus SNR

We then consider an overdetermined case where  $(N, P) = (7, 4)$  and our proposed method provides the ability to provide better estimation accuracy than other estimators in different SNRs. The true DOAs are  $\{\theta_1, \theta_2, \theta_3, \theta_4\} = \{-20^\circ, -10^\circ, 12^\circ, 24^\circ\}$ , where  $\{-20^\circ, -10^\circ\}$  is a group of coherent signals and  $\{12^\circ, 24^\circ\}$  is another group. The number for subarrays and snapshots is set to 3 and 100, respectively. The other simulation conditions are similar to Example 5.1. Moreover, the Cramér–Rao bound (CRB) [39,40] is also presented.

As observed in the simulation results of Figure 3, our proposed method can still achieve coherent DOA estimation when compared with the existing methods based on Toeplitz matrix reconstruction. This is because the array dimension for the Toeplitz methods is less than the number of sources, while our proposed method, based on Khatri–Rao subspace processing, employs a virtual array structure to extend the physical array aperture, which results in resolving more signals. Meanwhile, the Khatri–Rao processing also eliminates the color noise. This aligns with the theoretical analysis presented in Section 4.

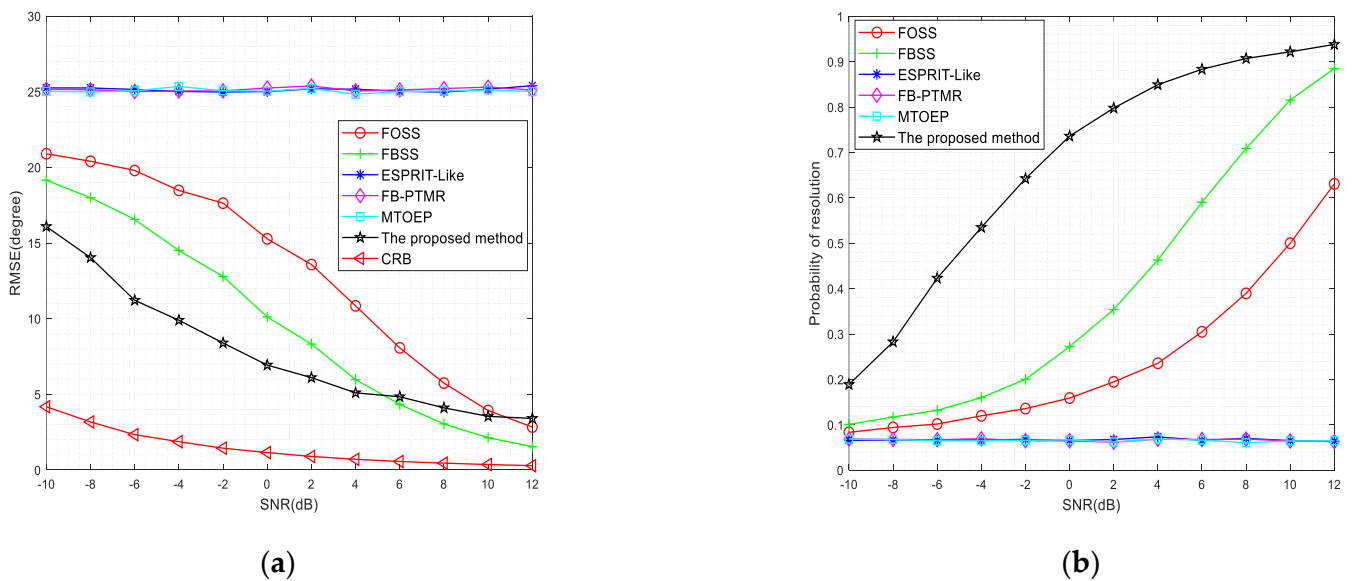


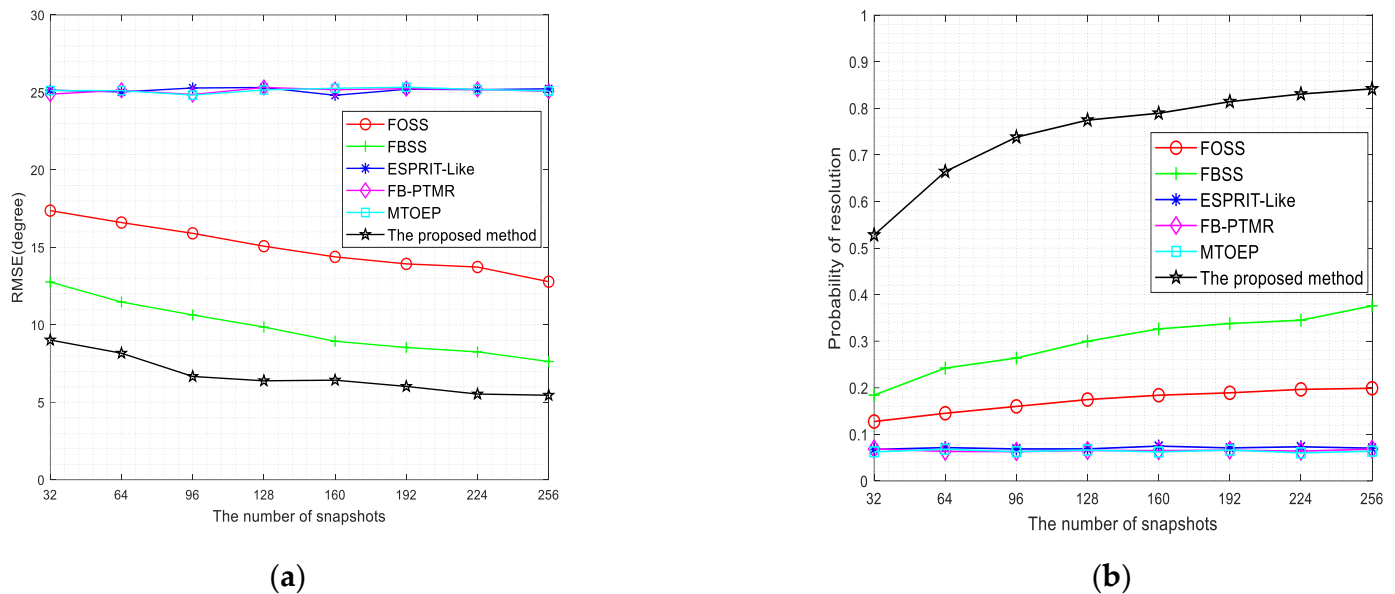
Figure 3. DOA estimation performance versus SNR. (a) RMSE versus SNR. (b) POR versus SNR.

Figure 3 also shows that when  $SNR \leq 6$  dB, our proposed method provides better estimation performance on accuracy and resolution. Meanwhile, the DOA estimation performance is closer to CRB than other methods. Furthermore, the proposed method can produce a slightly interior RMSE performance at higher SNRs than the FBSS method, but the resolution probability in our method obviously outperforms the FBSS method. Particularly when  $SNR = 0$  dB, our proposed algorithm improves estimation accuracy ( $RMSE \approx 7^\circ$ ) and resolution probability ( $POR \approx 74\%$ ) than that of other methods ( $RMSE \geq 10^\circ, POR \leq 27\%$ ).

### 5.3. Estimation Performance versus Snapshots

The DOA estimation performance concerning the snapshot numbers is also investigated. The simulation conditions are similar to those in Example 5.2, except that the snapshot number varies from 32 to 256 and the SNR is fixed at 0 dB.

Figure 4 illustrates that our proposed method provides good estimation accuracy over the entire snapshot regime. When compared with the other methods, our proposed method can realize the array aperture extension using the Khatri–Rao subspace processing. Thus, our proposed method yields better estimation accuracy and resolution under the same snapshot number. Figure 4 also shows that the DOA estimation performance for our proposed method is significantly improved faster than other methods as an increase in the number of snapshots. This is especially true for a low number of snapshots such as 96; our proposed method can provide better estimation accuracy ( $RMSE \approx 7^\circ$ ) than other methods ( $RMS \geq 11^\circ$ ). Moreover, the resolution of probability in our proposed method is about 74%, while those of the others are below 26%.



**Figure 4.** DOA estimation performance versus snapshot number. (a) RMSE versus snapshot number. (b) POR versus snapshot number.

5.4. Estimation Performance versus Angular Separation

We tested the estimation performance versus the angular separation. Two groups of coherent signals are also considered, which are set to  $\{-30^\circ, -30^\circ + \Delta\theta\}$  and  $\{0^\circ, 0^\circ + \Delta\theta\}$ , respectively. The angular separation  $\Delta\theta$  varies from  $2^\circ$  to  $18^\circ$ , and the snapshot number is set to 200. The other conditions are the same as those in Example 5.1.

From the simulation results as shown in Figure 5, we can conclude that our proposed method provides better estimation performance than that of other estimators across the entire angular separation regime. Compared to the FOSS and FBSS methods, our proposed method achieves the extension of the array physical aperture when combined with the Khatri–Rao subspace processing. Therefore, this will result in better estimation accuracy. Furthermore, Figure 5 also shows that when the angular separation is enlarged, the RMSEs of the spatial smoothing methods gradually approach and are still lower than our proposed method. Meanwhile, the resolution probability of our proposed method is also significantly improved. In particular, when the angular separation  $\Delta\theta = 18^\circ$ , the estimation accuracy of the FBSS is similar to our proposed method, while the resolution probability ( $POR \approx 90\%$ ) in our scheme is higher than that of the FBSS method ( $POR \approx 53\%$ ).

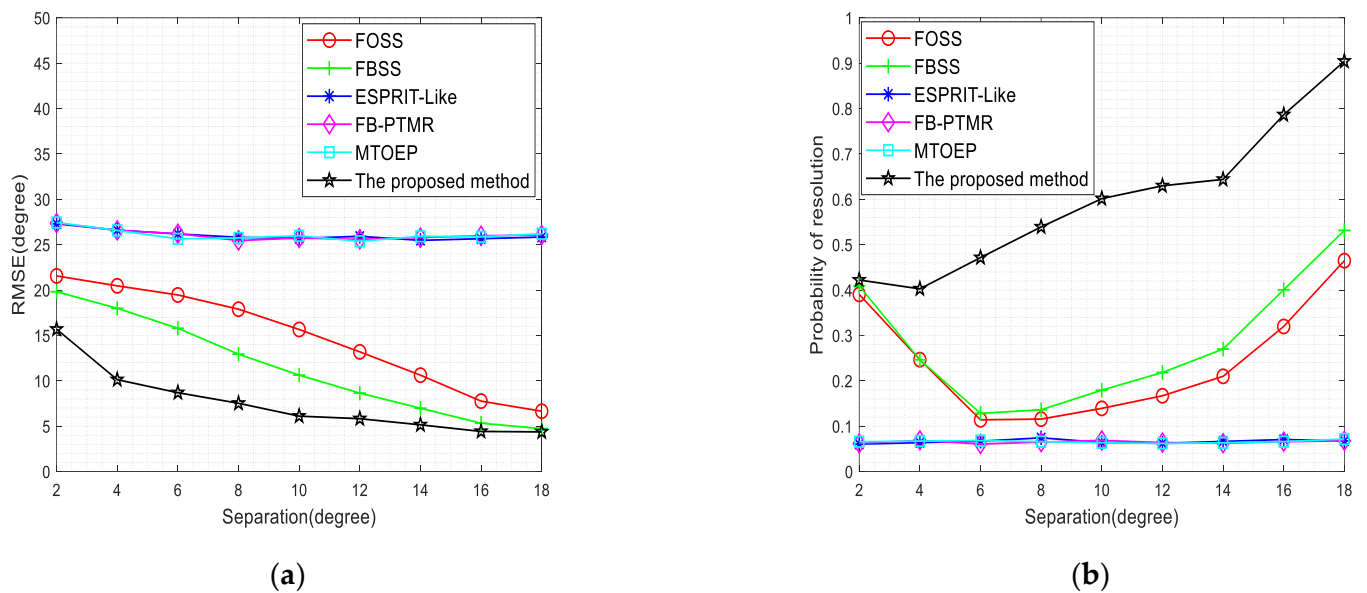


**Figure 5.** DOA estimation performance versus angular separation. (a) RMSE versus angular separation. (b) POR versus angular separation.

## 6. Conclusions

An enhanced ESPRIT-like method that combines Khatri–Rao product processing and Toeplitz reconstruction was proposed to solve the DOA estimation for coherent sources. The proposed method firstly constructs the Toeplitz matrix with full rank to achieve decorrelation. Then, the Khatri–Rao characteristic contained in the array response is inherently further employed to achieve the array aperture extension, which further provides the capability to identify more sources that can be resolved by the other methods. The numerical results confirm the validity of our proposed method. Furthermore, our analysis also demonstrates that the proposed method can produce better estimates of the DOA in cases of low snapshots, low SNR regime, and closely spaced sources.

**Author Contributions:** Conceptualization, B.Q.; Methodology, B.Q., X.L., D.D. and R.H.; Software, B.Q.; Validation, B.Q.; Formal analysis, X.L, D.D. and R.H.; Investigation, R.H.; Resources, B.Q. and X.L.; Data curation, D.D. and R.H.; Writing—original draft, B.Q. and R.H.; Writing—review& editing, Y.Z. All authors have read and agreed to the published version of the manuscript.

**Funding:** This research received no external funding.

**Data Availability Statement:** The data presented in this study are available on request from the corresponding author.

**Conflicts of Interest:** The authors declare no conflict of interest.

## References

1. Krim, H.; Viberg, M. Two decades of array signal processing research: The parametric approach. *IEEE Signal Process. Mag.* **1996**, *13*, 67–94. [[CrossRef](#)]
2. Godara, L.C. Application of antenna arrays to mobile communications. II. Beam-forming and direction-of-arrival considerations. *Proc. IEEE* **1997**, *85*, 1195–1245. [[CrossRef](#)]
3. Kim, S.; Oh, D.; Lee, J. Joint DFT-ESPRIT Estimation for TOA and DOA in Vehicle FMCW Radars. *IEEE Antennas Wirel. Propag. Lett.* **2015**, *14*, 1710–1713. [[CrossRef](#)]
4. Lee, H.; Ahn, J.; Kim, Y.; Chung, J. Direction-of-Arrival Estimation of Far-Field Sources Under Near-Field Interferences in Passive Sonar Array. *IEEE Access* **2021**, *9*, 28413–28420. [[CrossRef](#)]
5. Amin, M.G.; Wang, X.; Zhang, Y.D.; Ahmad, F.; Aboutanios, E. Sparse Arrays and Sampling for Interference Mitigation and DOA Estimation in GNSS. *Proc. IEEE* **2016**, *104*, 1302–1317. [[CrossRef](#)]
6. Yan, H.; Fan, H. On source association of DOA estimation under multipath propagation. *IEEE Signal Process. Lett.* **2005**, *12*, 717–720.

7. Xie, W.; Wen, F.; Liu, J.; Wan, Q. Source Association, DOA, and Fading Coefficients Estimation for Multipath Signals. *IEEE Trans. Signal Process.* **2017**, *65*, 2773–2786. [[CrossRef](#)]
8. Roy, R.; Kailath, T. ESPRIT-estimation of signal parameters via rotational invariance techniques. *IEEE Trans. Acoust. Speech Signal Process.* **1989**, *37*, 984–995. [[CrossRef](#)]
9. Schmidt, R. Multiple emitter location and signal parameter estimation. *IEEE Trans. Antennas Propag.* **1986**, *34*, 276–280. [[CrossRef](#)]
10. Shan, T.J.; Wax, M.; Kailath, T. On spatial smoothing for direction-of-arrival estimation of coherent signals. *IEEE Trans. Acoust. Speech Signal Process.* **1985**, *33*, 806–811. [[CrossRef](#)]
11. Pillai, S.; Kwon, B. Forward/backward spatial smoothing techniques for coherent signal identification. *IEEE Trans. Acoust. Speech Signal Process.* **1989**, *37*, 8–15. [[CrossRef](#)]
12. Choi, Y.-H. On conditions for the rank restoration in forward/backward spatial smoothing. *IEEE Trans. Signal Process.* **2002**, *50*, 2900–2901. [[CrossRef](#)]
13. Wen, J.; Liao, B.; Guo, C. Spatial smoothing based methods for direction-of-arrival estimation of coherent signals in nonuniform noise. *Digit. Signal Process.* **2017**, *67*, 116–122. [[CrossRef](#)]
14. Du, W.; Kirlin, R. Improved spatial smoothing techniques for DOA estimation of coherent signals. *IEEE Trans. Signal Process.* **1991**, *39*, 1208–1210. [[CrossRef](#)]
15. Pan, J.; Sun, M.; Wang, Y.; Zhang, X. An Enhanced Spatial Smoothing Technique with ESPRIT Algorithm for Direction of Arrival Estimation in Coherent Scenarios. *IEEE Trans. Signal Process.* **2020**, *68*, 3635–3643. [[CrossRef](#)]
16. Vincent, F.; Besson, O.; Chaumette, E. Approximate Unconditional Maximum Likelihood Direction of Arrival Estimation for Two Closely Spaced Targets. *IEEE Signal Process. Lett.* **2015**, *22*, 86–89. [[CrossRef](#)]
17. Yao, B.; Zhang, W.; Wu, Q. Weighted Subspace Fitting for Two-Dimension DOA Estimation in Massive MIMO Systems. *IEEE Access* **2017**, *5*, 14020–14027. [[CrossRef](#)]
18. Das, A. Deterministic and Bayesian Sparse Signal Processing Algorithms for Coherent Multipath Directions-of-Arrival (DOAs) Estimation. *IEEE J. Ocean. Eng.* **2019**, *44*, 1150–1164. [[CrossRef](#)]
19. Uehashi, S.; Ogawa, Y.; Nishimura, T.; Ohgane, T. Prediction of Time-Varying Multi-User MIMO Channels Based on DOA Estimation Using Compressed Sensing. *IEEE Trans. Veh. Technol.* **2019**, *68*, 565–577. [[CrossRef](#)]
20. Das, A.; Hodgkiss, W.S.; Gerstoft, P. Coherent Multipath Direction-of-Arrival Resolution Using Compressed Sensing. *IEEE J. Ocean. Eng.* **2017**, *42*, 494–505. [[CrossRef](#)]
21. Chen, H.; Hou, C.-P.; Wang, Q.; Huang, L.; Yan, W.-Q. Cumulants-Based Toeplitz Matrices Reconstruction Method for 2-D Coherent DOA Estimation. *IEEE Sens. J.* **2014**, *14*, 2824–2832. [[CrossRef](#)]
22. Shi, H.; Li, Z.; Liu, D.; Chen, H. Efficient method of two-dimensional DOA estimation for coherent signals. *EURASIP J. Wirel. Commun. Netw.* **2017**, *53*, 1–10. [[CrossRef](#)]
23. Han, F.-M.; Zhang, X.-D. An ESPRIT-like algorithm for coherent DOA estimation. *IEEE Antennas Wirel. Propag. Lett.* **2005**, *4*, 443–446.
24. Zhang, W.; Han, Y.; Jin, M.; Li, X.-S. An Improved ESPRIT-Like Algorithm for Coherent Signals DOA Estimation. *IEEE Commun. Lett.* **2020**, *24*, 339–343. [[CrossRef](#)]
25. Zhang, W.; Han, Y.; Jin, M.; Qiao, X. Multiple-Toeplitz Matrices Reconstruction Algorithm for DOA Estimation of Coherent Signals. *IEEE Access* **2019**, *7*, 49504–49512. [[CrossRef](#)]
26. Qi, B.B.; Li, W. An Improved Multiple-Toeplitz Matrices Reconstruction Algorithm for DOA Estimation of Coherent Signals. *Radioengineering* **2021**, *30*, 532–539. [[CrossRef](#)]
27. Qi, B. DOA estimation of the coherent signals using beamspace matrix reconstruction. *Signal Process.* **2021**, *191*, 108349. [[CrossRef](#)]
28. Ma, W.; Hsieh, T.; Chi, C. DOA estimation of quasi-stationary signals via Khatri-Rao subspace. In Proceedings of the IEEE International Conference on Acoustics, Speech and Signal Processing, Taipei, Taiwan, 19–24 April 2009; pp. 2165–2168.
29. Ma, W.-K.; Hsieh, T.-H.; Chi, C.-Y. DOA Estimation of Quasi-Stationary Signals With Less Sensors Than Sources and Unknown Spatial Noise Covariance: A Khatri-Rao Subspace Approach. *IEEE Trans. Signal Process.* **2010**, *58*, 2168–2180. [[CrossRef](#)]
30. Fang, Y.; Zhu, S.; Gao, Y.; Zeng, C. DOA Estimation for Coherent Signals With Improved Sparse Representation in the Presence of Unknown Spatially Correlated Gaussian Noise. *IEEE Trans. Veh. Technol.* **2020**, *69*, 10059–10069. [[CrossRef](#)]
31. Viberg, M.; Stoica, P.; Ottersten, B. Maximum likelihood array processing in spatially correlated noise fields using parameterized signals. *IEEE Trans. Signal Process.* **1997**, *45*, 996–1004. [[CrossRef](#)]
32. Wang, Y.; Trinkle, M.; Ng, B.W.H. Two-stage DOA estimation of independent and coherent signals in spatially coloured noise. *Signal Process.* **2016**, *128*, 350–359. [[CrossRef](#)]
33. Mei, D.; Shouhong, Z.; Xiangdong, W.; Huanying, Z. A High Resolution Spatial Smoothing Algorithm. In Proceedings of the 2007 International Symposium on Microwave, Antenna, Propagation and EMC Technologies for Wireless Communications, Hangzhou, China, 16–17 August 2007; pp. 1031–1034.
34. Bachl, R. The forward-backward averaging technique applied to TLS-ESPRIT processing. *IEEE Trans. Signal Process.* **1995**, *43*, 2691–2699. [[CrossRef](#)]
35. Qi, B.; Zhang, H.; Zhang, X. Time-frequency DOA estimation of chirp signals based on multi-subarray. *Digit. Signal Process.* **2021**, *113*, 103031. [[CrossRef](#)]
36. Huang, L.; Long, T.; Mao, E.; So, H.C. MMSE-Based MDL Method for Accurate Source Number Estimation. *IEEE Signal Process. Lett.* **2009**, *16*, 798–801. [[CrossRef](#)]

37. Chang, C.-I.; Du, Q. Estimation of Number of Spectrally Distinct Signal Sources in Hyperspectral Imagery. *IEEE Trans. Geosci. Remote Sens.* **2004**, *42*, 608–619. [[CrossRef](#)]
38. Belouchrani, A.; Amin, M.G. Time-frequency MUSIC. *IEEE Signal Process. Lett.* **1999**, *6*, 109–110. [[CrossRef](#)]
39. Stoica, P.; Nehorai, A. MUSIC, maximum likelihood, and Cramer-Rao bound. *IEEE Trans. Acoust. Speech Signal Process.* **1989**, *37*, 720–741. [[CrossRef](#)]
40. Stoica, P.; Nehorai, A. Performance comparison of subspace rotation and MUSIC methods for direction estimation. *IEEE Trans. Signal Process.* **1991**, *39*, 446–453. [[CrossRef](#)]

**Disclaimer/Publisher’s Note:** The statements, opinions and data contained in all publications are solely those of the individual author(s) and contributor(s) and not of MDPI and/or the editor(s). MDPI and/or the editor(s) disclaim responsibility for any injury to people or property resulting from any ideas, methods, instructions or products referred to in the content.